STM JOURNALS

Journal of
Experimental & Applied Mechanics

ISSN: 2230-9845 (Online)
ISSN: 2321-516X (Print)
Volume 16, Issue 2, 2025
May–August
DOI (Journal): 10.37591/JoEAM

https://journals.stmjournals.com/joeam

Research JoEAM

A Method of Mesh Deformation for Flow Analysis Around Oscillating Bodies

Phyong Guk Paek, Yun Hyok Kim, Sol Song Pak*, Yong Chol Pak, Chong Il Hong

Abstract

In general, high-speed rotating machines are subjected to complex phenomena due to various reasons, such as increased noise and strong vibration due to dynamic unbalance, which affect the dynamic motion of rotating machines and are necessarily a problem to overcome. Therefore, it is necessary to have a mathematical model to simulate it, and a strong tool to solve the constructed model. Using fluid-structure coupling techniques, which are currently a powerful technique for solving practical problems, great progress can be made in simulating the hoop phenomenon and studying the dynamic characteristics of high-speed rotating machines. Unless the fluid structure problems are solved in combination, accurate results cannot be produced, which will be a strong challenge for design and research. Especially in such a motion with strong nonlinearity, early success cannot necessarily be expected without using powerful tools and techniques. The plata phenomenon and various nonlinear fluid-solid interaction problems typically considered in rotating machinery and airframes require essentially a flow analysis around a vibrating body. In general, to solve the fluid-solid interaction problem, the flow field analysis in the computational domain, which is changing due to the motion of solids, and the deformation of solids due to the action of hydrodynamic forces, must be considered simultaneously. In this study, a method of mesh deformation suitable for the motion of a body is proposed in the analysis of the flow field around a vibrating body. The integral form of the two-dimensional Euler equation in the variable computational domain is discretized using the finite volume method. Boundary conditions on the object surface are realized by mirror reflection in a local coordinate system fixed to the object surface to satisfy the impermeability condition through the object boundary. The far-field boundary conditions were applied at the outer boundary. To provide the boundary conditions correctly, the nodes of the body boundary must always be placed at the body boundary during the calculation. Also, to maintain the mesh quality, the velocity of the nodal movement at a position close to the object boundary must be greater than that at a far location. And the nodes of the outer boundary must be fixed. To determine the travel speed of the grid nodes, one algebraic equation is solved at each grid node. This can greatly reduce the computational effort in the computational domain, which is changed due to the motion of the object. The accuracy was verified by compressible flow field analysis around a two-dimensional oscillating blade. In this study, the flow around the oscillating Naca0012 blade is analyzed.

***Author for Correspondence**
Sol Song Pak
E-mail: SS.PAK@star-co.net.kp

Faculty of Mechanics, Department of Mechanics, Kim Il Sung University, Taesong District, Pyongyang, Democratic People's Republic of Korea

Received Date: May 16, 2025
Accepted Date: July 01, 2025
Published Date: July 26, 2025

Citation: Phyong Guk Paek, Yun Hyok Kim, Sol Song Pak, Yong Chol Pak, Chong Il Hong. A Method of Mesh Deformation for Flow Analysis Around Oscillating Bodies. Journal of Experimental & Applied Mechanics. 2025; 16(2): 35–42p.

Keywords: Vibration, airfoil, fluid analysis, angle of attack, sign

INTRODUCTION

Generally, POD is applied to supersonic aeroelastic problems with subsonic flow and static impact properties [1–15]. POD has also been used for wing design of low-speed flying vehicles [16].

Computers using POD ROM can generate data at very fast rates with flow control over incompressible flow fields [1, 14, 15]. Recently,

there are many examples of moving impact problems of transonic flow fields to study the dynamics of high speed rotating machines.

This study addresses the problem of how to use POD/ROM in a two-dimensional high-speed flow field. Dynamic impulse is an important index used in reduced order methods. When the shock wave moves uniformly, linearization of the shock flow field to some shock wave position will produce an error. Because of these difficulties, reduced order methods do not have a significant effect on the motion of strongly impacted objects [17, 18].

Analyzing the literature, one of the methods for the accurate solution of strong moving shock waves is the domain decomposition technique, which can be used to accurately exploit the POD/ROM [19]. Since POD/ROM constructs a flow field from a linear superposition of a set of modes, all spatial locations of the computational mesh require a special representation. The use of the POD/ROM/DD method can overcome these drawbacks. The aim of this study is to extend the one-dimensional (1-D) POD/ROM/DD method to the analysis of fast, metastable, and two-dimensional flow fields, thereby increasing its accuracy, causing dimensionality reduction, and reducing computational costs.

The change in inlet Mach number and angle of attack (AOA) resulted in a metastable motion of a strong shock wave propagating from the head of the wedge. The blunt-body problem provides a two-dimensional flow field with a moving shock wave that is documented and understood. This problem provides an ideal test bench to identify and solve implementation, stability, and accuracy problems.

A review of POD is provided by a discussion of the subspace mapping method used to explicitly integrate reduced order variables into time integration. Next, a semi-implicit formulation of subspace projection is provided, including a description of an optimization-based solver used to connect overlapping domain parts.

Finally, we give two results.

1. The first results are related to POD/ROM/DD using a fully ordered model within the shock domain.
2. The second result is related to POD/ROM/DD using POD/ROM within the impact zone.

This case experienced some difficulties as described by Mortara *et al*. [20]. The results for both cases are used to evaluate the feasibility of POD/ROM/DD.

DISCRETIZATION OF THE SYSTEM OF EQUATIONS

The integral form of the two-dimensional Euler equation in the changing computational domain is as follows [2, 3]:

$$\frac{\partial}{\partial t}\iint_{\Omega} W dxdy + \int_{\partial\Omega}\left(En_x + Gn_y\right)dl = 0 \tag{1}$$

In Eq. (1), Ω is the time-varying computational domain due to the motion of the body and n_x, n_y are the unit-outward normal vector components of the changing border $\partial\Omega$. W is the conservative variable vector, E is the X-direction flow vector, and G is the Y-direction flow vector.

$$W = \begin{pmatrix} \rho \\ \rho u \\ \rho v \\ e \end{pmatrix}, E = \begin{pmatrix} \rho U \\ \rho U u + p \\ \rho U v \\ eU + pu \end{pmatrix}, G = \begin{pmatrix} \rho V \\ \rho V u \\ \rho V v + p \\ eV + pv \end{pmatrix}$$

In the above equation ρ is the density of the fluid, u and v are the X and Y-directional components of the fluid velocity, p is the pressure of the fluid, and e is the total energy per unit volume. On the other hand, $U = u - x_t$ $V = v - y_t$, x_t and y_t are respectively the mesh travel velocities in X and Y-directions.

The pressure p is given by the equation of state of the perfect gas $p = (\gamma - 1)\rho e$. With the discretization using the finite volume method, Eq. (1) is given as follows:

$$(\Omega_i W_i)^{n+1} - (\Omega_i W_i)^n + \Delta t \sum_j^{n_i} (F_{ij}) dl_{ij} = 0 \tag{2}$$

In Eq. (2), $F_{ij} = \left(En_x + Gn_y\right)_{ij}$ is the numerical flow rate vector, Ω_i represents the volume of the ith element, dl_{ij} represents the interface length between the i th element and its adjacent element j, and the superscript n represents the time step.

Including mesh motion, the eigenvalues of the system of equations are different from the eigenvalues without mesh motion.

Now consider the flow rate vector as follows:

$$F = \bar{F} + v_{mesh}\mathrm{W} \tag{3}$$

In Eq. (3), $\overline{F}$ is the flow rate vector without mesh motion and $v_{mesh} = x_t n_x + y_t n_y$ is the normal velocity of mesh motion.

Expressing the flow Jacobian from Eq. (3) is as follows:

$$A = \frac{\partial F}{\partial W} = \frac{\partial F}{\partial W} + \frac{\partial}{\partial W}(v_{mesh} W) = R\Lambda\mathrm{L} + v_{mesh} I =$$
$$= R\Lambda\mathrm{L} + v_{mesh} RIL = R(\Lambda - v_{mesh} I)L \tag{4}$$

In Eq. (4), R is the right eigenvector matrix, L is the left eigenvector matrix, and $\boldsymbol{\Lambda} = diag(u_n, u_n, u_n + c, u_n - c)$ is the eigenvalue matrix. Here u_n is the normal velocity of the fluid at the element boundary and c is the local acoustic velocity.

As shown in Eq. (4), the eigenvalues vary with the normal velocity of the mesh. Boundary conditions on the body surface are realized by mirror reflection in a local coordinate system fixed to the body surface to satisfy the impermeability condition through the body boundary. The far-field boundary conditions were applied at the exterior boundary.

MESH DEFORMATION METHOD

As the body moves, the computational mesh must be correspondingly deformed. In the study by Hwang and Yang [2], the mesh in the computational domain is considered as a spring system and the mesh deformation is realized by the following static equilibrium equation:

$$\Delta x_j = \frac{\sum_{l=1}^{n_j} K_l \cdot \Delta y_l}{\sum_{l=1}^{n_j} K_l}, \Delta y_j = \frac{\sum_{l=1}^{n_j} K_l \cdot \Delta y_l}{\sum_{l=1}^{n_j} K_l} \tag{5}$$

In Eq. (5), K_l is the spring modulus and n_j is the number of all adjacent nodes surrounding node j.

As can be seen from Eq. (5), in the study by Hwang and Yang [2], the displacement of the nodes was determined by solving the system of equations with iteration so that the force balance at each time is satisfied by considering the computational mesh as a spring system.

This requires the solution of an additional set of equations to solve the system of governing equations, which requires more computational effort. We propose a more efficient method to maintain the quality of the deformed mesh with less computational effort.

In order to provide the boundary conditions correctly, the nodes of the body boundary must always be at the body boundary during the calculation. Also, in order to maintain the mesh quality, the moving velocity of the nodes at locations close to the body boundary must be higher than that at far locations. And the nodes of the exterior boundary must be fixed.

Hence, the moving speed of the nodes can be expressed as:

$$\begin{cases} x_t = D_1 \cdot u_0/(D_0 + D_1) \\ y_t = D_1 \cdot v_0/(D_0 + D_1) \end{cases} \tag{6}$$

In Eq. (6), D_0 is the distance from the node under consideration to the nearest point of the body boundary, and D_1 is the distance to the nearest point of the exterior boundary. u_0 and v_0 are the moving velocity components of the body boundary point closest to the node under consideration.

The position of the nodes' movement is determined by integrating Eq. (6). As can be seen from Eq. (6), one algebraic equation is solved at each grid node to determine the moving velocity of the grid nodes. This can greatly reduce the computational effort in the computational domain, which changes due to the motion of the body.

Figure 1 shows the original mesh and the deformed mesh based on Eq. (6). From the Figure 1, it can be seen that the mesh deformation proceeds reasonably in accordance with the motion of the body.

COMPUTATIONAL RESULTS

In the study we analyzed the flow around the oscillating Naca0012 blade. The oscillation type is harmonic vibration as follows:

$$\alpha(t) = \alpha_0 + \alpha_{max} \cdot sin(\omega t) \tag{7}$$

$\alpha_0 = 0.016°$, $\alpha_{max} = 2.51°$, $k = \omega\overline{C}/(2U_\infty) = 0.0814$, $M_\infty = 0.755$.

In the equation 7, α is the angle of attack, ω is the angular frequency, k is the reduced frequency, $\overline{C}$ is the characteristic length, and U_∞ and M_∞ are the absolute value of the flow velocity at the exterior boundary and Mach number.

Experimental results on this computational example are presented in the study by Hwang and Yang [2]. Figures 2 and 3 show the pressure coefficient curves with non-dimensional chord length $X/\overline{C}$ at different angles of attack. Figure 2(a–d) is the result of the increase first and then decrease of the angle of attack α in the positive sign, and Figure 3(a–d) is the result of the increase in its absolute value first and then decrease of the angle of attack in the negative sign.

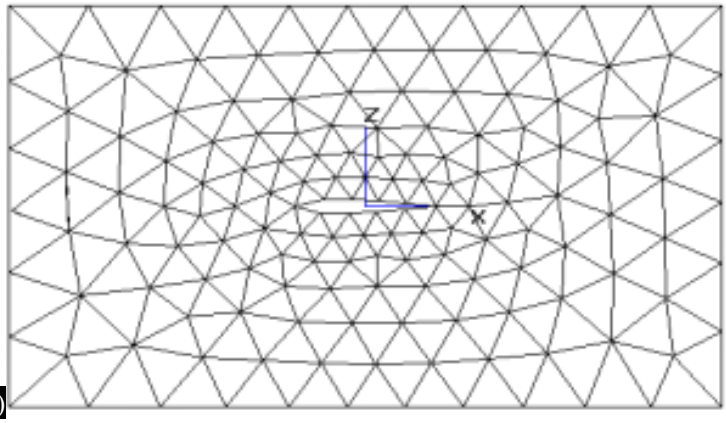

(a)

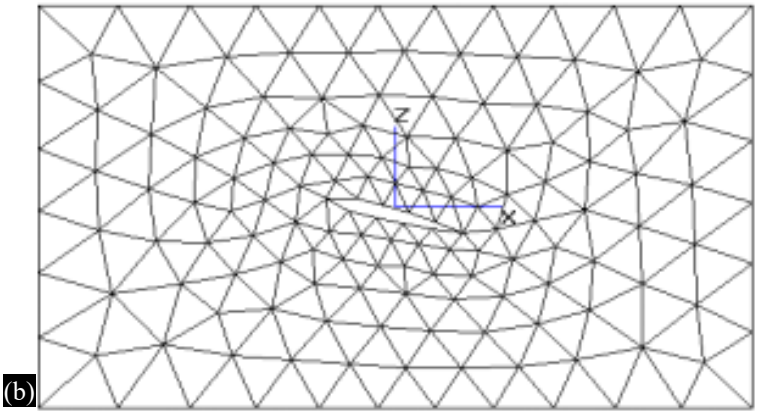

Figure 1. Mesh deformation. (a) original mesh, (b) deforming mesh.

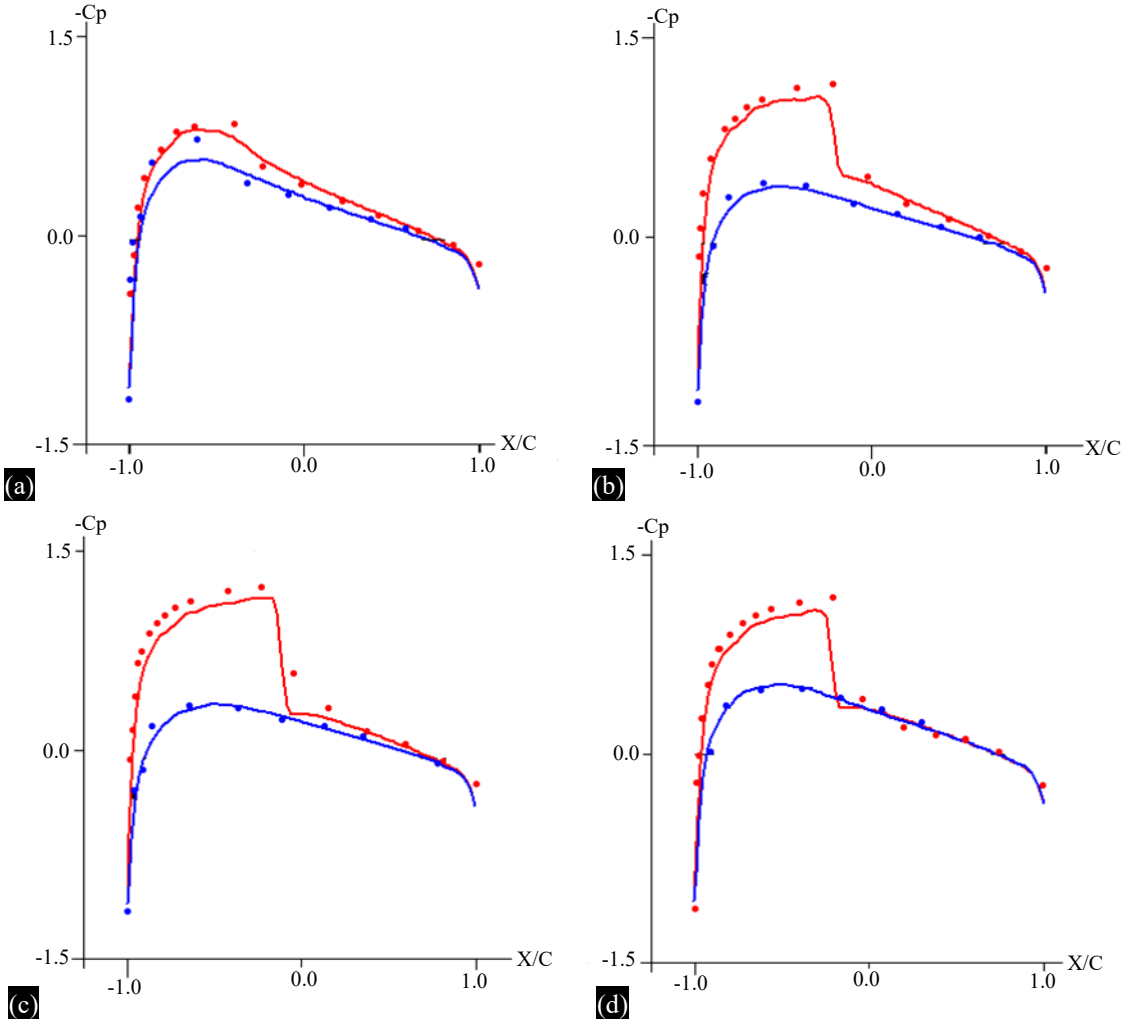

Figure 2. Lift coefficient at different angles of attack (When the angle of attack has a positive sign), experimental value. (a) α=–1.09º, (b) α=–2.34º, (c) α=–2.01º, (d) α=–0.52º.

When the sign of the angle of attack changes, the sign of the pressure coefficients of the upper and lower surfaces of the blade also changes. It can be seen from the figure that the position of the shock wave on the blade surface and the pressure distribution are almost symmetrical with the oscillation of the blade on the lower and upper surfaces.

Figure 4 shows the lift coefficient curve with angle of attack. As α increases and decreases, the values of lift coefficient at the same angle of attack are different, which can be attributed to the dynamic effect of blade motion on lift.

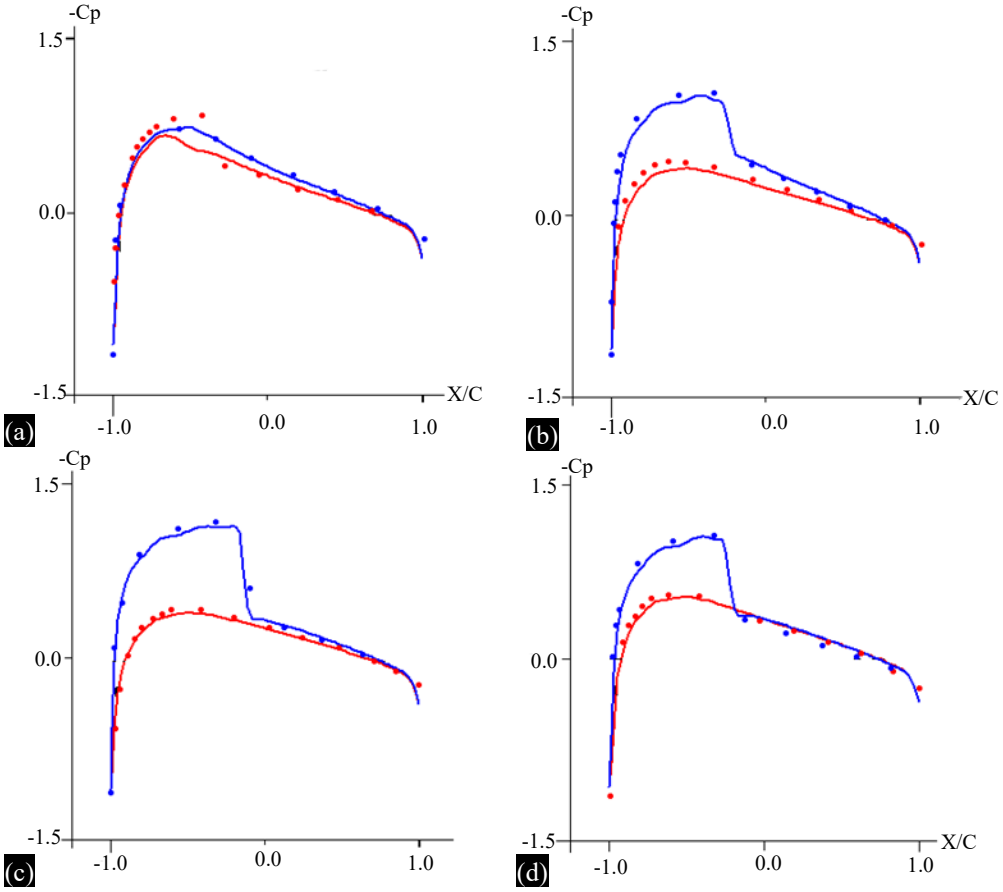

Figure 3. Lift coefficient at different angles of attack (When the angle of attack has a negative sign), experimental value. (a) α=–1.25º, (b) α=–2.41º, (c) α=–2.0º, (d) α=–0.54º.

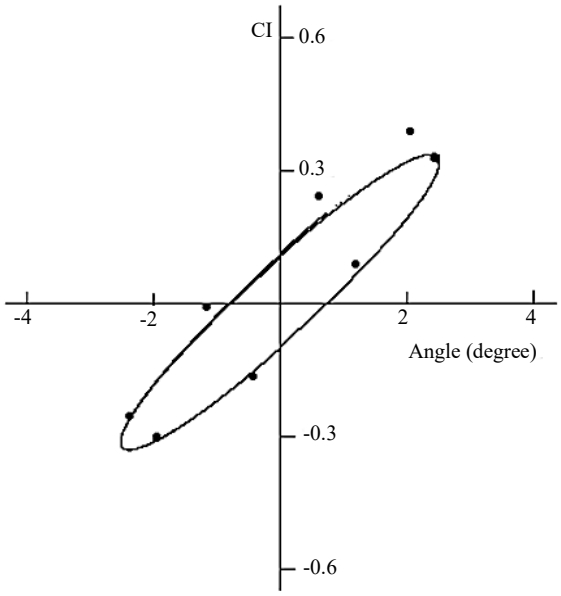

Figure 4. Lift coefficient with angle of attack, experimental value.

The lower part of the closed symmetric lift curve is when the speed of change of the angle of attack is positive, i.e. when the angle of attack increases, and the upper part is when the speed of change of the angle of attack is negative, i.e. when the angle of attack decreases.

CONCLUSION

As the results show, when the speed of change of angle of attack is negative, the lift acting on the blade is bigger. Compared with the experimental results, the computational results show a relatively accurate analysis of the flow field around the blade during its oscillation.

Acknowledgement

This study was funded by Faculty of Dynamics, Kim Il Sung University.

Conflict of Interest

None (separate file).

REFERENCES

1. Dowell Earl H. A modern course in aeroelasticity. In: Solid Mechanics and Its Applications. Cham: Springer; 2004; 116.
2. Hwang CJ, Yang SY. Locally Implicit Total Variation Diminishing Schemes on Mixed Quadrilateral-Triangular Meshes. AIAA Journal. 1993; 31(11): 2008–2015.
3. Kershaw David S, Prasad Manoj K. 3D Unstructured mesh ALE hydrodynamics with the upwind discontinuous finite element method. Comput Methods Appl Mech Eng. 1998; 158(1–2): 81–116.
4. Beran PS, Huttsell LJ, Buxton BJ, Noll C, Osswald G. Computational aeroelastic techniques for viscous flow. In: CEAS/AIAA/ICASE/NASA Langley International Forum on Aeroelasticity and Structural Dynamics, Williamsburg, VA. 1999 Jun 22–25.
5. Dowell EH. Eigenmode analysis in unsteady aerodynamics: Reduced-order analysis. Am Inst Aeronaut Astronaut J. 1996; 34(8): 1578–83.
6. Dowell EH, Hall KC. Modeling of fluid–structures interaction. Ann Rev Fluid Mech. 2001; 33: 445–90.
7. Dowell EH, Hall KC, Thomas J, Florea R, Epureanu B, Heeg J. Reduced order models in unsteady aerodynamics. In: AIAA/ASME/ASCE/AHS/ASC Structures, Structural Dynamics and Materials Conference, St. Louis, MO. 1999 Apr 12–15.
8. Epureanu BI, Dowell EH, Hall KC. A parametric analysis of reduced order models of potential flows in turbomachinery using proper orthogonal decomposition. 2001-GT-0434. In: Proceedings of ASME Turbo-Expo 2001, New Orleans, Louisiana. 2001 Jun 4–7.
9. Epureanu BI, Hall KC, Dowell EH. Reduced order models of unsteady transonic viscous flows in turbomachinery. J Fluids Struct. 2000; 14(8): 1215–34.
10. Epureanu BI, Hall KC, Dowell EH. Reduced order models in turbomachinery using inviscid–viscous coupling. J Fluids Struct. 2001; 15(2): 255–76.
11. Florea R, Hall KC, Dowell EH. Eigenmode analysis and reduced order modeling of unsteady transonic full potential flow around isolated airfoils. In: CEAS/AIAA/ICASE/NASA Langley International Forum on Aeroelasticity and Structural Dynamics, Williamsburg, VA. 1999 Jun 22–25.
12. Hall KC, Thomas JP, Dowell EH. Reduced-order modeling of unsteady small-disturbance flows using a frequency domain proper orthogonal decomposition technique. In: AIAA 99-0655, 37th Aerospace Sciences Meeting and Exhibit, Reno, NV. 1999 Jan 11–15.
13. Holmes P, Lumley J, Berkooz G. Turbulence, coherent structures, dynamical systems and symmetry. Cambridge, MA: Cambridge University Press; 1996.
14. Ito K, Ravindran SS. A reduced-order method for simulation and control of fluid flows. J Computat Phys. 1998; 143(2): 403–25.
15. Kunisch K, Volkwein S. Control of the Burgers equation by a reduced-order approach using proper orthogonal decomposition. J Optim Theory Appl. 1999; 102: 345–71.

16. LeGresley PA, Alonso JJ. Airfoil design optimization using reduced order models based on proper orthogonal decomposition. In AIAA 2000-2545, Fluids 2000 Conference and Exhibit, Denver, CO. 2000 Jun.
17. Lucia DJ. Reduced order modeling for high speed flows with moving shocks. PhD thesis. USA: Air Force Institute of Technology, School of Engineering and Management; 2001.
18. Lucia DJ, Beran PS, King PI. Reduced order modeling of an elastic panel in transonic flow. In: AIAA 2002-1594, 43rd AIAA/ASME/ASCE/AHS Structures, Structural Dynamics, and Materials Conference, Denver, CO. 2002 Apr 22–25.
19. Lucia DJ, King PI, Beran PS, Oxley ME. Reduced order modeling for a one-dimensional nozzle flow with moving shocks. In: AIAA 2001-2602, 19th AIAA Computational Fluid Dynamics Conference, Anaheim, CA. 2001 Jun.
20. Mortara SA, Slater JC, Beran PS. An optimal proper orthogonal decomposition technique for the computation of nonlinear panel flutter. In: AIAA 2000-1936. 2000.

